Macedonian Journal of Chemistry and Chemical Engineering, Vol. **44**, No. 1, pp. 39–52 (2025)

MJCCA9 – 919

ISSN 1857-5552
e-ISSN 1857-5625

Received: March 9, 2025
Accepted: April 21, 2025

DOI: 10.20450/mjcce.2025.3098
Original scientific paper

DFT ANALYSIS OF FENETHYLLINE (CAPTAGON): INVESTIGATING ITS INTERACTION WITH GRAPHENE AS A POTENTIAL ADSORBENT

Valbonë Mehmeti[1], Vllaznim Mula[2], Moussa Djibrilla Maiga[3,4], Mahamadou Seydou[3,4], Omar Dagdag[5], Avni Berisha[6*], Savaş Kaya[7]

[1]*Faculty of Agriculture and Veterinary, University of Prishtina, Prishtina, Republic of Kosovo*
[2]*University "Fehmi Agani" in Gjakova, Republic of Kosovo*
[3]*Centre de Calcul de Modélisation et de Simulation (CCMS), Université des Sciences, des Techniques et des Technologies de Bamako, Mali*
[4]*Université Paris Cité, CNRS, ITODYS, 75013 Paris, France*
[5]*Department of Mechanical Engineering, Gachon University, Seongnam 13120, Republic of Korea*
[6]*Department of Chemistry, Faculty of Natural and Mathematics Science, University of Prishtina, 10000 Prishtina, Republic of Kosovo*
[7]*Sivas Cumhuriyet University, Faculty of Science, Department of Chemistry, 58140 Sivas, Turkey*
avni.berisha@uni-pr.edu

Fenethylline, commonly known as Captagon, is a stimulant with amphetamine-like properties that has gained notoriety due to its widespread illicit use, particularly in conflict zones. Its ease of synthesis and environmental persistence necessitate effective remediation strategies. This study investigates the adsorption potential of graphene (G) for Captagon removal using a multi-scale computational approach, including density functional theory (DFT), Monte Carlo (MC), and molecular dynamics (MD) simulations. The interaction between Captagon and graphene was analyzed in both perpendicular and parallel adsorption configurations. The results indicate that the parallel orientation exhibits superior adsorption stability, with an adsorption energy of –51.15 kcal mol^{-1}, primarily driven by π–π stacking interactions. Frontier molecular orbital (FMO) analysis further reveals significant alterations in graphene's electronic properties upon Captagon adsorption, with noticeable shifts in the Highest Occupied Molecular Orbital (HOMO) and Lowest Unoccupied Molecular Orbital (LUMO) energy levels and bandgap (E_{gap}). The molecular dynamics simulations confirm the stability of the Captagon-graphene complex, reinforcing graphene's potential as a viable adsorbent. These findings highlight graphene's efficiency in Captagon removal, suggesting its broader applicability in water purification and environmental remediation strategies.

Keywords: density functional theory; Monte Carlo simulation; molecular dynamics simulation; Captagon; graphene; adsorption

DFT-АНАЛИЗА НА ФЕНЕТИЛИН (КАПТАГОН): ИСПИТУВАЊЕ НА НЕГОВАТА ИНТЕРАКЦИЈА СО ГРАФЕН КАКО ПОТЕНЦИЈАЛЕН АТСОРБЕНТ

Фенетилин, познат и како каптагон, е стимуланс со својства слични на амфетамините, кој стекна лоша репутација поради неговата широка нелегална употреба, особено во конфликтни зони. Неговата лесна синтеза и неразградливост во животната средина бараат ефикасни стратегии за отстранување. Оваа студија ја испитува потенцијалната атсорпција на графен (G) за отстранување на каптагон користејќи повеќеслоен пристап во компјутерското моделирање, вклучувајќи ги теоријата на функционалот на густина (DFT), симулациите Монте Карло (MC) и симулацијата со молекуларна динамика (MD). Заемодејството помеѓу каптагон и графенот беше анализирано во перпендикуларни и паралелни конфигурации на атсорпција. Резултатите укажуваат дека паралелната ориентација покажува поголема стабилност на атсорпција, со енергија

на атсорпција од –51.15 kcal mol^{-1}, главно поттикната од π–π интеракции. Анализата на граничните молекулски орбитали (FMO) дополнително открива значителни промени во електронските својства на графенот по атсорпцијата на каптагон, со забележливи поместувања на енергетските нивоа на највисоко пополнетата молекулска орбитала (HOMO) и најниско непополнетата молекулска орбитала (LUMO), како и на енергетскиот процеп (E_{gap}). Симулациите со молекуларна динамика ја потврдуваат стабилноста на комплексот каптагон-графен, зацврстувајќи го потенцијалот на графенот како ефикасен атсорбент. Овие наоди ја истакнуваат ефикасноста на графенот во отстранувањето на каптагон, сугерирајќи поширока примена во прочистувањето на вода и во стратегиите за еколошка ремедијација.

Клучни зборови: теорија на функционалот на густина; симулација Монте Карло; симулација со молекуларна динамика; каптагон, графен

1. INTRODUCTION

The emergence of new psychoactive substances, along with the reappearance of older ones when newer alternatives are scarce, presents a significant public health challenge. These designer drugs are frequently used as substitutes to mimic the effects of traditional controlled substances during periods of unavailability. One such substance, Captagon (chemically known as fenethylline, structure shown in Scheme 1), is a synthetic psychoactive stimulant that has garnered notoriety for its widespread abuse, particularly across the Middle East.

Originally developed in the 1960s for medical applications, Captagon has since become a widely misused drug, especially in Saudi Arabia and conflict zones such as Syria.[1–6] Captagon's pharmacological properties are particularly complex, as it combines the stimulant effects of amphetamines with the bronchodilator properties of theophylline. This combination enhances energy levels, induces euphoria, and improves cognitive and physical performance.[3–6] Users often experience heightened confidence and aggression, making it especially appealing to individuals engaged in combat. Its prevalence in war-affected regions has raised significant concerns about its role in fueling violence and exacerbating instability.[3,7]

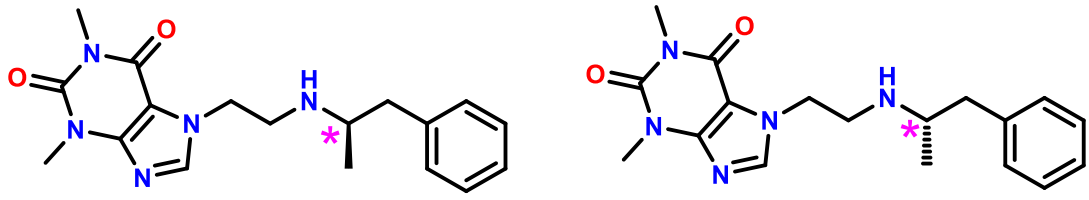

Scheme 1. The structure of fenethylline (Captagon) exists as two enantiomers, (*R*)-fenethylline and (*S*)-fenethylline, each containing a chiral center, indicated by a pink asterisk

The production and trafficking of Captagon have evolved significantly, with clandestine laboratories now operating in Southern Europe and the Middle East, particularly in countries like Syria.[8] Captagon's prevalence in the region has led to the annual seizure of millions of tablets, highlighting the scale of its misuse and the challenges faced by law enforcement.

Graphene,[9] a single layer of carbon atoms arranged in a two-dimensional honeycomb lattice, has garnered significant attention due to its remarkable mechanical, thermal, and electrical properties.[10] Its unique structure contributes to exceptional characteristics such as high electron mobility, impressive thermal conductivity, and substantial mechanical strength, making it a promising candidate for various applications in electronics, materials science, and nanotechnology.[10–13] Graphene and its derivatives, particularly graphene oxide (GO), have emerged as promising materials for drug delivery systems[14] due to their unique physical and chemical properties. The high surface area of graphene allows for significant molecule adsorption,[15] which is crucial for enhancing the efficacy of therapeutic agents.

Studies have demonstrated that graphene-based nanocarriers can achieve high loading capacities for various anticancer drugs, including doxo-

rubicin and cisplatin, making them effective in targeted drug delivery applications.[10,16,17] Graphene's ability to adsorb drug molecules is influenced by several factors, including the nature of the drug, the functionalization of the graphene surface, and the specific interactions involved. For instance, studies have shown that the adsorption energy of drugs varies significantly depending on their molecular structure and the distance from the graphene surface. Gong et al.[18] demonstrated that the vertical distances between graphene and various anticancer drug molecules correlate with their adsorption energies, indicating that greater distances lead to weaker adsorption capacities.[19] This finding aligns with the general understanding that π–π interactions and hydrophobic effects play crucial roles in the adsorption of aromatic compounds on graphene.[15,20]

The consequences of Captagon extend beyond public health and safety to serious environmental hazards. The production of this drug, which is illegal in most countries, leads to the uncontrolled release of hazardous chemicals into the soil and waterways, thereby polluting all biodiversity. Moreover, discarded or degraded Captagon pills may leach psychoactive substances into the ecosystem, threaten animal life, and further disrupting fragile environmental balances. These pollutants, though difficult to eliminate, can still be mitigated through methods that, while not entirely efficient, remain effective in preventing irreversible damage. One such approach is the use of graphene-based materials, which possess outstanding surface area and strong adsorption capabilities.

Graphene's unique properties can be leveraged in the design of advanced filtration systems necessary for capturing and eliminating Captagon-related pollutants, thereby protecting the environment from further harm. Although concerns regarding Captagon's environmental impact are growing, little is known about its adsorption efficiency on graphene-based materials. The use of state-of-the-art computational techniques enables the modeling of Captagon adsorption, combining methods from quantum mechanics with those from molecular mechanics. Such advanced computational models will provide key insights into the interaction between Captagon and graphene surfaces at the atomic level, focusing on quantifying interaction strength, adsorption energy, and molecular orientation relative to the substrate.

In this study, we employ computational chemistry to examine graphene effectiveness as an adsorbent for Captagon removal, laying the foundation for further testing and future applications in environmental remediation.

2. THEORETICAL CALCULATIONS

2.1. *Molecular models*

The interaction of the Captagon molecule with graphene was investigated using a finite 9 × 9 zigzag graphene nanostructure (shown in Figure 1), carefully selected to ensure a sufficiently large surface area capable of accommodating the entire Captagon molecule without significant edge effects. This model size allows for an accurate representation of molecular adsorption while minimizing artificial boundary constraints, thereby preserving the intrinsic electronic and structural properties of both the molecule and the graphene sheet. The structure of Captagon was downloaded from PubChem database.[21] Prior to density functional theory (DFT) calculations, the structure underwent a conformer search using Orca 6.0 software.[22–24]

2.2. *Conformer search*

The computational approach employed the GFN1-xTB Hamiltonian,[25] as implemented in the ORCA 6.0 software. This tight-binding quantum chemical method provides an efficient balance between computational cost and accuracy, making it particularly suitable for optimizing geometries of large molecular systems and accurately capturing non-covalent interactions. For this calculation, the system was modeled as neutral with a singlet spin state. An integral accuracy threshold of 0.2 ensured robust Self-Consistent Field (SCF) convergence within a tolerance of 2.0×10^{-6} Eh. The computation was executed using 164 parallel threads, significantly enhancing performance. Convergence stability was further improved through Broyden damping set at 0.4.

2.3. *Monte Carlo*

The adsorption behavior of Captagon molecules was studied using the Adsorption Locator module in Materials Studio. A simulated annealing approach was employed with 100,000 loading steps and 30 heating cycles, each containing 100,000 steps, resulting in a total number of 3,000,000 randomly generated configurations. The Dreiding force field was used,[26] with electrostatic interactions computed using an atom-based summation method and a cubic spline truncation method, applying a cutoff distance of 18.5 Å. The Van der Waals interactions were treated similarly.

The Monte Carlo (MC) simulation was conducted both in the gas phase and a simulated aque-

ous environment. In the latter case, 250 water molecules were incorporated to ensure complete hydration of the graphene surface. The number of water molecules was determined based on the total surface area of graphene, ensuring a realistic representation of the hydration environment.

2.4. *Molecular dynamics (MD)*

The molecular dynamics (MD) simulation was conducted using the Forcite module in Materials Studio. The initial geometry for the molecular dynamics (MD) simulation was selected based on the adsorption configuration with the highest interaction energy, as determined in the preceding Monte Carlo (MC) simulation. This approach ensures that the MD simulation starts from the most stable and energetically favorable adsorption pose, allowing for a more accurate assessment of system dynamics and interaction behavior over time.

The simulation employed an canonical ensemble (NVT), where the number of particles (*N*), volume (V), and temperature (*T*) are kept constant (T = 298 K), controlled via the Nose thermostat[27] with a Q ratio of 0.01. A Dreiding force field was used to describe intermolecular interactions, with electrostatic and Van der Waals interactions computed using an atom-based summation method and a cubic spline truncation method with a cutoff distance of 18.5 Å. Hydrogen bond interactions were also considered, using a 4.5 Å cutoff distance. The simulation was performed with a time step of 1.0 fs over 2,000,000 steps, corresponding to a total duration of 2000 ps (2 ns).

2.5. *DFT calculations (DFT)*

Density functional theory (DFT) calculations were performed using the DMol³ module[28] within the BIOVIA Materials Studio package. The electronic structure calculations were conducted to determine the energy and electronic properties of the system. The computational setup and parameters were chosen to ensure accuracy and convergence while maintaining computational efficiency.

The calculations were performed without imposing symmetry constraints, to allow full structural relaxation. A double numerical plus polarization (DNP) basis set[29] was employed to provide an accurate representation of the wavefunction. No pseudopotentials were applied, meaning that all-electron calculations were performed. The M11L meta-GGA functional[30] was used to describe the exchange-correlation effects, as it offers a reliable balance between accuracy and computational cost for systems involving weak interactions.

The self-consistent field (SCF) convergence criterion[31] was set to 1.0×10^{-6} e Å^{-3} for charge density. To enhance SCF stability, charge and spin mixing parameters were set to 0.2 and 0.5, respectively. Pulay direct inversion in the iterative subspace (DIIS) with six iterations was employed to accelerate convergence. The system was treated with unrestricted spin polarization, allowing for an independent treatment of alpha and beta spin electrons. The total system charge was set to neutral (0) to reflect experimental conditions.

The global cutoff radius for atomic orbitals was set to 3.7 Å, ensuring accurate representation of wavefunctions and interactions. A hexadecapole auxiliary density expansion was used for numerical integration. The integration grid was set to 'fine' to balance computational cost and accuracy.

2.6. *Calculations via the general utility lattice program (GULP)*

General utility lattice program (GULP)[32,33] is a computational tool designed for simulating materials across various boundary conditions, including 0-D (molecules and clusters), 1-D (polymers), 2-D (surfaces, slabs, and grain boundaries), and 3-D (periodic solids). Unlike molecular dynamics, GULP prioritizes analytical solutions through lattice dynamics whenever feasible. Due to its efficiency in handling large systems, GULP serves as a valuable alternative to density functional theory (DFT) when computational cost is a concern. Geometry optimization was performed using ReaxFF 6.0 force field.[34]

3. RESULTS AND DISCUSSION

3.1. *Conformer search*

3.1.1. *Global optimization and conformer analysis*

The global optimization procedure identified 178 conformers within 3 kcal mol^{-1} of the global minimum energy, which was calculated to be –75.879529 Eh (Figure 2).

The conformational analysis revealed an entropy contribution (S_{conf}) of 8.86 cal mol^{-1} K^{-1} and a free energy correction (G_{conf}) of –1.78 kcal mol^{-1}, indicating moderate flexibility among the conformers. This range of low-energy conformers suggests that Captagon molecule has several accessible configurations, which may influence its dynamic behavior and potential applications in various environments.

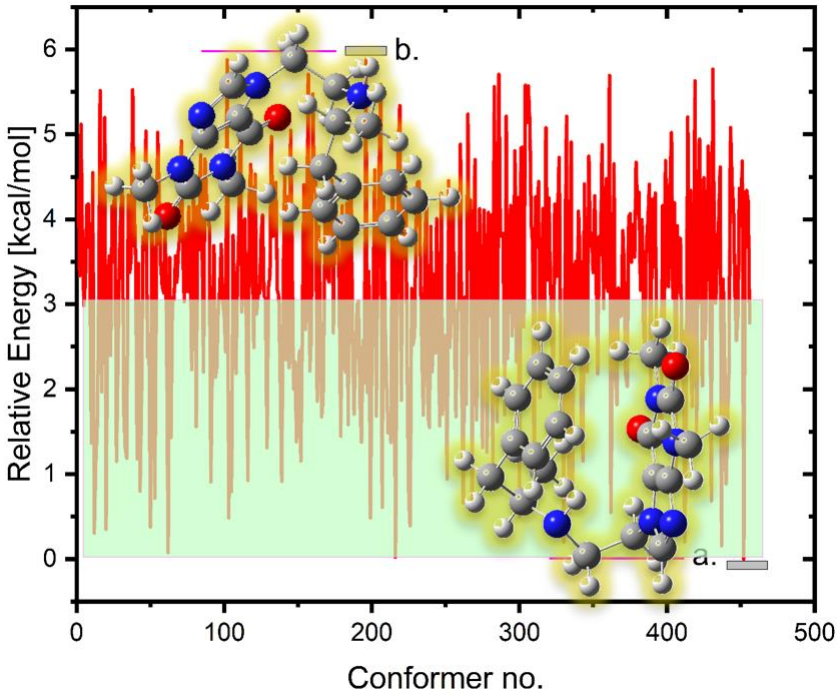

Fig. 1. Conformer energy landscape and the lowest (a) and the highest (b) energy conformers

3.2. *Monte Carlo and molecular dynamics simulations*

Monte Carlo calculations are widely used to investigate and gain deeper insights into adsorption phenomena occurring on various surfaces. These simulations provide a powerful statistical approach to modeling adsorption processes by accounting for molecular interactions, surface heterogeneity, and thermodynamic fluctuations.[35–39] In this study, the Monte Carlo (MC) simulation results, as depicted in Figure 2, demonstrate that Captagon molecules spontaneously adsorb onto the graphene surface.

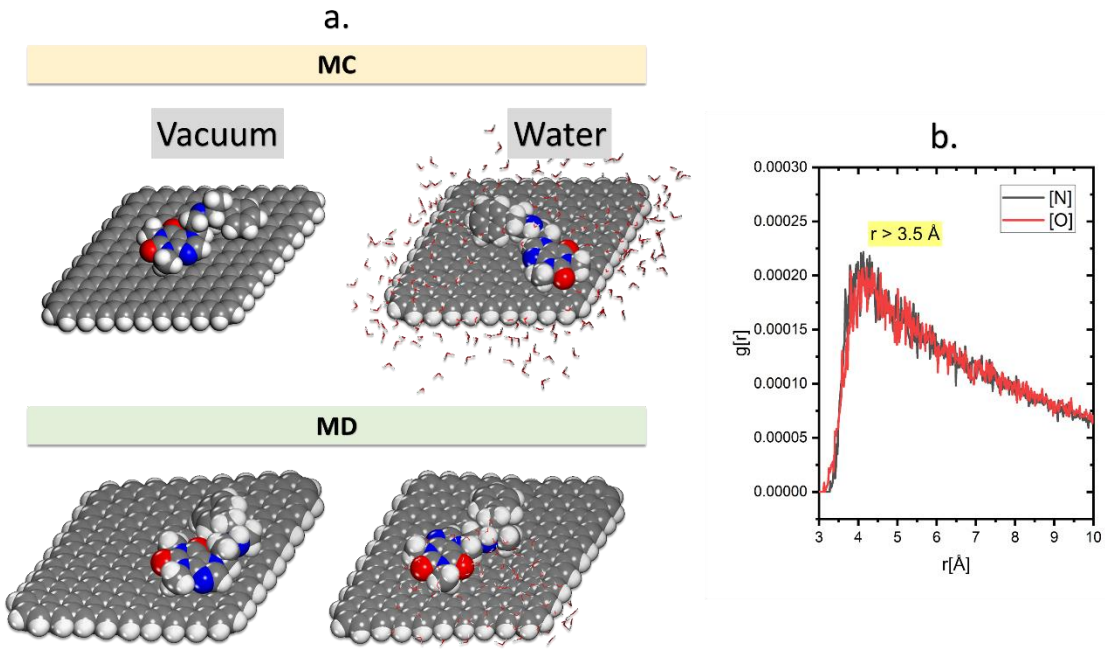

Fig. 2. (a) Lowest energy configurations of the Captagon on the surface obtained from Monte Carlo (MC) and molecular dynamics (MD) simulations under vacuum and aqueous conditions. (b) Radial distribution functions (RDF) g(r) for nitrogen and oxygen atoms of the Captagon relative to the surface atoms of graphene, indicating predominant interaction distances beyond 3.5 Å.

This spontaneous absorption is evidenced by the significantly negative adsorption energy values, which indicate a thermodynamically favorable interaction between Captagon and the graphene substrate. The pronounced exothermic nature of the adsorption process suggests strong intermolecular forces, likely driven by π–π interactions between the aromatic rings of Captagon and the delocalized π-electron system of graphene.

T a b l e 1

MC output values for the absorption of Captagon molecules onto the graphene surface

Structures	Adsorption energy	Rigid adsorption energy	Deformation energy	Water: dEad/dNi
Pose 1 (in water)	–61.51	–51.15	27.32	–2.33
Pose 1(in vacuum)	–41.52	–41.45	–0.07	–

The Monte Carlo (MC) simulation results reveal a significantly stronger adsorption of Captagon onto the graphene surface in an aqueous environment compared to vacuum conditions. The rigid adsorption energy – defined as the energy change upon adsorption of a molecule (Captagon) onto a surface (graphene) without allowing structural relaxation of either the adsorbate or the adsorbent – follows the same trend, with values of −51.15 kcal mol^{-1} in water and −41.45 kcal mol^{-1} in vacuum. These results further support the enhanced binding affinity in the presence of water molecules, likely due to solvation effects and favorable intermolecular interactions.

Additionally, the deformation energy in water (27.32 kcal mol^{-1}) is substantially higher than in vacuum (–0.07 kcal mol^{-1}), suggesting that Captagon undergoes structural adjustments to optimize its interaction with graphene in an aqueous environment. The energy contribution analysis highlights that Captagon itself plays a dominant role in adsorption, contributing –61.51 kcal mol^{-1} in water and –41.52 kcal mol^{-1} in vacuum, while water has a minor stabilizing effect (–2.33 kcal mol^{-1}). These findings collectively indicate that graphene exhibits a significantly higher affinity for Captagon in aqueous environments, reinforcing its potential as an efficient adsorbent for Captagon detection and removal in water-based systems.

Molecular dynamics (MD) simulations are widely regarded as a more accurate representation of adsorption dynamics, providing a time-resolved perspective on molecular interactions.[35,40–42] In this study, MD results further confirm that the Captagon molecule remains adsorbed on the graphene surface throughout the entire simulation trajectory, regardless of the presence or absence of solvent molecules (water). This persistent adsorption highlights the strong intermolecular interactions between Captagon and graphene, demonstrating the molecule's high surface affinity. Notably, the stability of adsorption, even in aqueous environments, indicates that solvation effects do not significantly disrupt the binding process.

In the radial distribution function (RDF) graph, the presence and position of peaks at specific distances from the surface provide crucial insights into the adsorption mechanism occurring on the surface.[37,43–45] A peak appearing within the range of 1 to 3.5 Å indicates chemisorption, where strong covalent or electrostatic interactions are dominant. Conversely, RDF peaks occurring at distances greater than 3.5 Å suggest physisorption, which is primarily governed by Van der Waals forces.

In this study, RDF peaks for the oxygen (O) and nitrogen (N) atoms of the Captagon molecule are observed at distances below 3.5 Å from the graphene surface. This distance, combined with the significantly negative adsorption energy values, strongly suggests that Captagon interacts forcefully with graphene. The proximity of these atoms to the surface indicates a pronounced interaction, potentially involving charge transfer or π–π stacking, further reinforcing the molecule's strong affinity for graphene.

These findings highlight graphene's potential as an efficient adsorbent for Captagon, with implications for its detection and removal in various applications.

3.3. *Density functional theory (DFT)*

In this study, the computed DFT parameters are presented in Table 2. The interaction energies of the Captagon molecule adsorbed on a 9 × 9 graphene sheet were calculated using density functional theory (DFT) and presented in Figure 3 [Computational details: A comprehensive summary of all simulation settings and parameters (including those from DFT, Monte Carlo, MD, and GULP optimizations) is provided in Table S1 of the Supporting Information].

T a b l e 2

MC output values for interaction of Captagon molecule onto graphene surface

System	HOMO [eV]	LUMO [eV]	Dipole [Debye]	ΔE [eV]	Fermi Level [eV]	Electroneg-ativity [eV]	Chemical Hardness [eV]
Captagon	–5.949	–1.871	4.4678	–	–3.9100	3.9100	2.039
G (9x9)	–4.318	–4.222	0.1062	–	–4.2700	4.2700	0.048
Pose 1	–4.293	–4.198	1.4846	0.096	–4.2455	4.2455	0.0475
Pose 2	–4.244	–4.147	6.4386	0.051	–4.1955	4.1955	0.0485
Pose 3	–4.307	–4.213	0.9887	0.061	–4.2600	4.2600	0.0470
Pose 4	–4.293	–4.198	2.2417	0.002	–4.2455	4.2455	0.0475

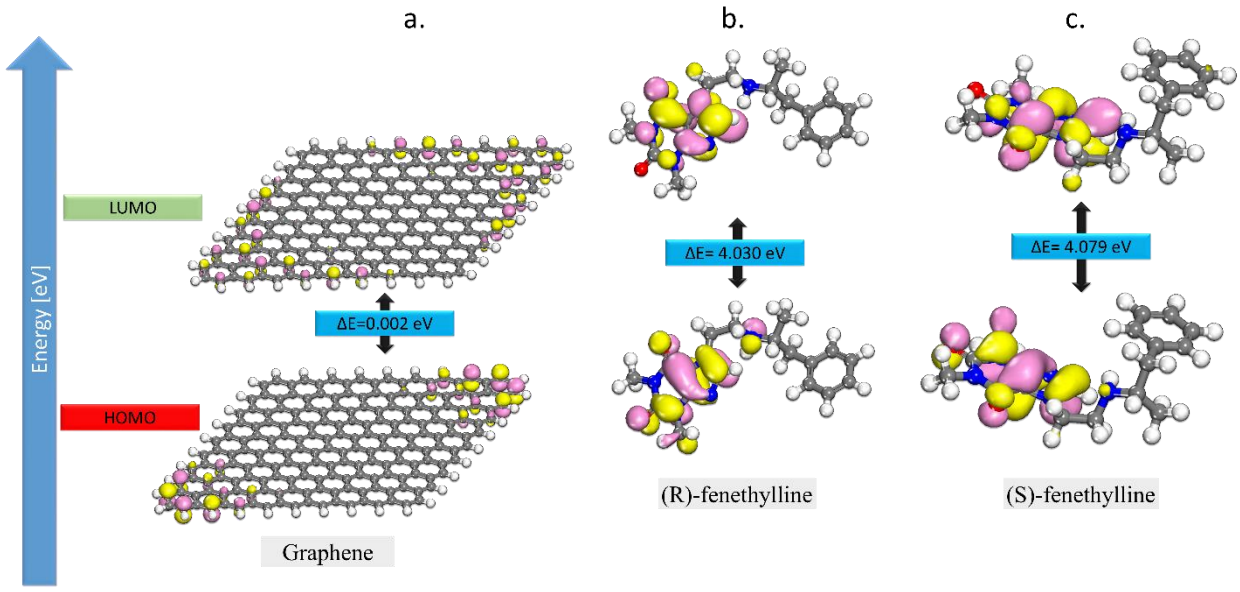

Fig. 3. Highest Occupied Molecular Orbital **(**HOMO) and Lowest Unoccupied Molecular Orbital (LUMO) energy levels for the optimized structures of: (a) graphene, (b) (*R*)-fenethylline, and (c) (*S*)-fenethylline.

The interaction energy (ΔE) was determined using the following equation:

$$E_{\text{interaction}} = E_{\text{complex}} - (E_{\text{Graphene}} + E_{\text{Captagon}}) \quad (1)$$

where E_{Complex} is the total energy of the Captagon-graphene system for each pose (P1 to P4); E_{Graphene} is the energy of the isolated graphene sheet; and E_{Captagon} is the energy of the isolated Captagon molecule.

The interaction energies between graphene and both (*R*)- and (*S*)-enantiomers of Captagon were evaluated based on the lowest-energy (most favorable) adsorption configurations obtained from structural optimization. The interaction energy of the graphene||(*R*)-Captagon system was calculated to be −39.53 kcal mol^{-1}, whereas the graphene||(*S*)-Captagon system exhibited a slightly less favorable interaction energy of −37.65 kcal mol^{-1}. This energy difference of 1.88 kcal mol^{-1} indicates that the (*R*)-enantiomer binds more strongly to the graphene surface, potentially due to more favorable π–π stacking interactions and steric complementarity with the 2D surface.

Further insight into these interactions is provided through an analysis of the dipole moments and frontier molecular orbitals of the isolated and adsorbed species. The isolated (*R*)-Captagon molecule possesses a dipole moment of 3.9979 D, while the (*S*)-enantiomer exhibits a higher dipole moment of 4.9707 D. Upon adsorption onto graphene, the dipole moments decrease to 1.4861 D for the graphene||(*R*)-Captagon system and 2.2203 D for the graphene||(*S*)-Captagon system. This decrease reflects partial charge delocalization into the graphene surface, along with polarization-induced reorganization of the molecular charge distribution, and suggests slightly different adsorption geometries for the two enantiomers.

In terms of electronic structure, the HOMO–LUMO energy gap of the isolated (*R*)-Captagon was found to be 4.03 eV, compared to 4.08 eV for the (*S*)-Captagon, indicating comparable intrinsic electronic reactivity. The pristine graphene sheet exhibited HOMO and LUMO levels at −4.319 eV and −4.317 eV, respectively, highlighting its narrow bandgap nature. Upon interaction with Captagon, notable shifts in the orbital energies were observed.

For the graphene||(*R*)-Captagon system, the HOMO shifted to −4.293 eV and the LUMO to −4.198 eV, whereas in the graphene||(*S*)-Captagon system, these values were slightly higher at −4.285 eV (HOMO) and −4.191 eV (LUMO). These shifts reflect enhanced electronic coupling and moderate charge transfer between the drug molecule and the graphene substrate in both cases.

In contrast, Pose 2 and Pose 3, where (*R*)-Captagon is oriented perpendicularly to the surface, exhibit weaker interactions, with Pose 3 having the weakest interaction energy of only –1.88 kcal mol^{-1}. These results suggest that different adsorption orientations lead to varying degrees of interaction strength, which may be influenced by factors such as π–π interactions and van der Waals forces between the Captagon molecule and the graphene surface.[15,46] The relatively short interaction distances of Captagon ring atoms (Fig. 4), particularly in the planar geometry of the (*R*)-Captagon molecule (Pose 1 and Pose 4), play a crucial role in enhancing the adsorption strength. In these configurations, the close proximity of the carbon to the graphene surface facilitates strong π–π interactions, which significantly contribute to the stability of the adsorbed complex. This enhanced interaction, coupled with van der Waals forces, explains the higher adsorption energies observed for these poses (Pose 1: –39.53 kcal mol^{-1}, Pose 4: –38.91 kcal mol^{-1}).

In contrast, the increased intermolecular distances observed in the perpendicular orientations (Pose 2 and Pose 3) result in reduced adsorption strength, primarily due to the loss of extended π–π conjugation between (*R*)-Captagon (hereafter referred to as Captagon) and the graphene surface.

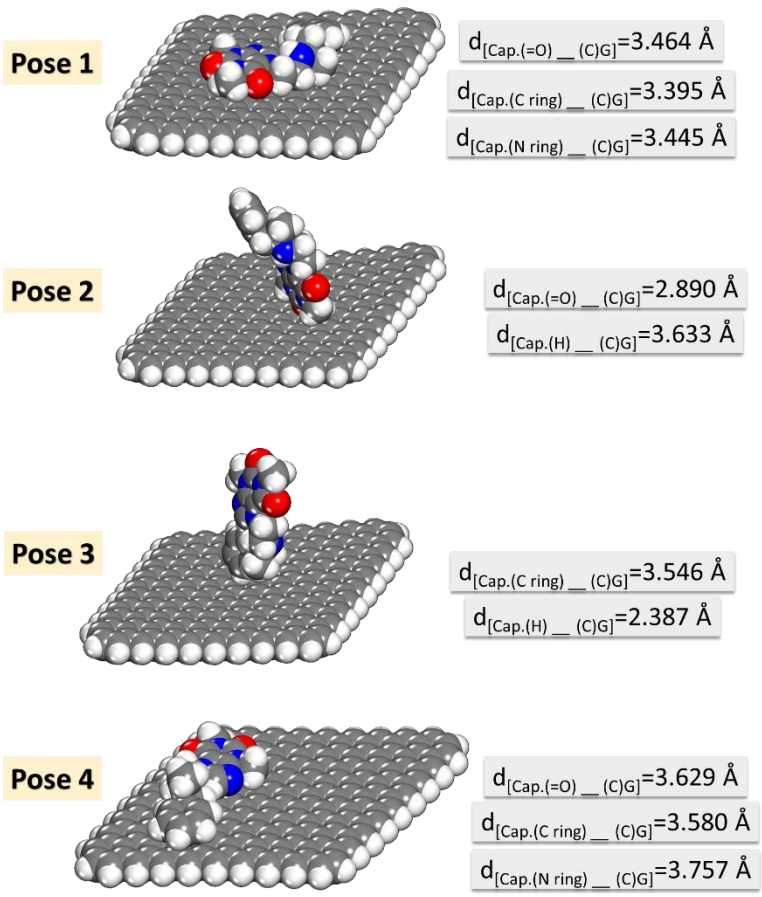

Fig. 4. Optimized geometries and selected bond distances between key interacting atoms of the (*R*)-Captagon molecule adsorbed on the graphene surface in four different configurations (Pose 1 to Pose 4)

Additionally, the surface area of interaction plays a crucial role, with planar orientations (Pose 1 and Pose 4) exhibiting larger contact areas that enhance interaction strength, whereas perpendicular orientations (Pose 2 and Pose 3) result in reduced contact and weaker interactions.[47]

Vertical adsorption of the Captagon molecule (Poses 2 and 3) produces a significantly higher average dipole moment (3.71 Debye) compared to planar adsorption geometries (1.48 Debye), indicating that vertical configurations lead to a more asymmetric charge distribution.

Planar adsorption poses have slightly lower HOMO and LUMO energies compared to vertical poses, but the difference is minimal. The absence of a strong difference between planar and vertical poses indicates that the fundamental electronic properties remain largely unaffected by adsorption geometry.

This slight difference suggests that molecular orbital energies are not significantly affected by the orientation. The atomic charge distribution in Captagon presented in Figure 5 highlights the role of electronegative atoms, particularly oxygen and nitrogen, as primary adsorption sites due to their significantly negative Mulliken charges.[48,49] Specifically, oxygen atoms (O1: –0.689; O2: –0.682) exhibit strong electronegativity, enabling them to engage in robust electrostatic interactions with the graphene surface, potentially enhancing adsorption stability. Additionally, nitrogen atoms (N3: –0.637; N5: –0.695; N6: –0.566; N7: –0.545) contribute substantial electron density, making them viable sites for both π–π stacking interactions and charge-transfer mechanisms with graphene.[50] These interactions are particularly relevant for tuning the electronic properties of the adsorbed system.

Conversely, carbon atoms within the aromatic rings (C9: 0.617; C10: 0.692; C11: 1.006) exhibit a slightly positive charge, increasing their affinity for graphene's delocalized π–electron system. The Mulliken charge distribution in graphene exhibits minor variations, with carbon atoms ranging from –0.252 to 0.120. These fluctuations indicate localized electron density differences, influencing graphene's adsorption capabilities. Positively charged carbon atoms can engage in π–π interactions with electron-rich regions of adsorbates, while negatively charged carbon sites (approximately –0.252) serve as potential interaction sites for electropositive species. This π–π stacking interaction enhances adsorption strength and promotes molecular stabilization on the graphene surface.[51,52]

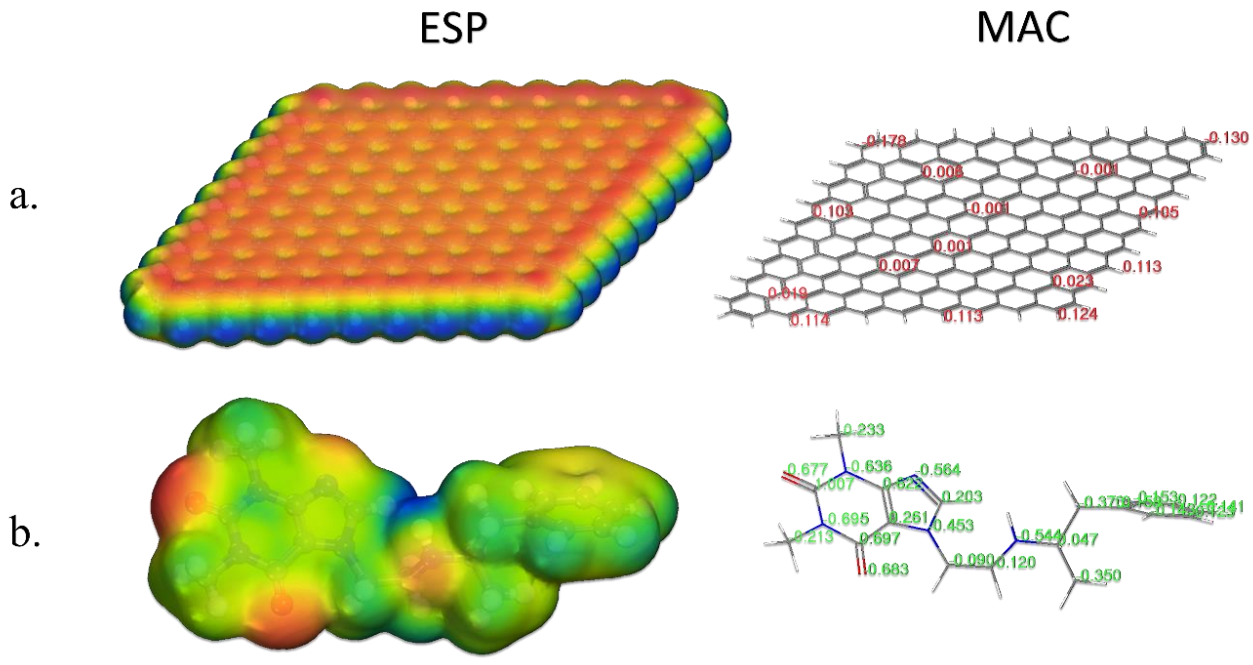

Fig. 5. Electrostatic potential (ESP) and Mulliken atomic charges (MAC) values for the optimized structures of: (a) graphene and (b) (R)-Captagon.

3.3.1. *Non-Covalent interaction (NCI) analysis of Captagon on graphene: π–π interactions*

The NCI-RDG (reduced density gradient) analysis enhances our understanding of interactions within a system by identifying and characterizing non-covalent interactions, whether occurring within a single molecule or between multiple molecules. This approach allows for the determination of interaction types, shedding light on their role in the system's behavior.

To visualize these interactions, we analyzed the RDG, which provides a spatial representation of where and how these forces manifest. To generate and visualize the results, we used the Multiwfn[53] and VMD programs[54] to create colored RDG scatter plots and 3D isosurfaces, as shown in Figure 6.

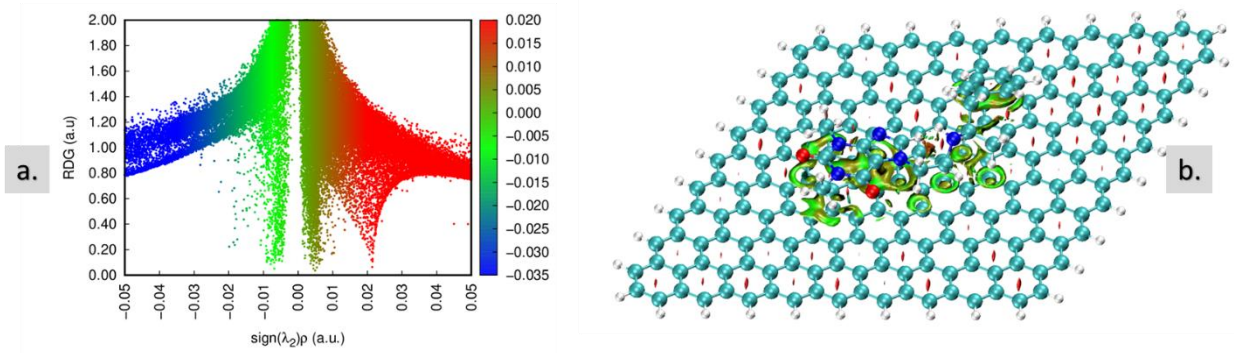

Fig. 6. (a) Scatter plot of the reduced density gradient (RDG) versus sign(λ₂)ρ, generated to identify and classify non-covalent interactions present in the Captagon–graphene system. The color scale represents the electron density (ρ) values associated with interaction types. (b) Three-dimensional visualization of RDG isosurfaces mapped onto the Captagon–graphene complex in Pose 1. The colored isosurfaces (blue, green, and red) represent regions of attractive, weak van der Waals, and steric repulsive interactions, respectively.

To analyze the nature and strength of non-covalent interactions (NCIs) between the Captagon molecule and the graphene surface, we employed the reduced density gradient (RDG) method. In our NCI analysis, we set the isosurface value at 0.5, with an RDG range spanning from 0.020 to –0.035 atomic units (a.u.). This approach enables differentiation between stabilizing and destabilizing interactions by evaluating the sign of the second eigenvalue (λ_2) of the Hessian matrix, multiplied by the electron density. Essentially, this method provides insight into both the curvature and electron density distribution of interactions, offering a quantitative measure of their strength and nature.

Figure 6 presents a comprehensive visualization of these non-covalent interactions through a combination of a 2D scatter plot and 3D RDG isosurface densities.[55–58] The RDG scatter plot reveals multiple interaction spikes, categorized into three distinct regions based on the values of sign(λ_2)ρ and are color-coded accordingly: *Highly Attractive Interactions (Blue Region)* – This region corresponds to strong attractive forces, primarily involving hydrogen bonding, characterized by negative sign(λ_2)ρ values. *Repulsive Interactions (Red Region)* – Associated with positive sign(λ_2)ρ values, this region indicates steric repulsion. In this case, steric hindrance is primarily observed at the phenyl rings of the graphene surface. This repulsion arises due to overlapping electron clouds, preventing excessive molecular overlap and helping to maintain structural integrity. The presence of these repulsive forces suggests that while Captagon's phenyl rings align with the graphene surface, they do not completely penetrate its electron density, thus preserving a balanced interaction. *Weak van der Waals Interactions (Green Region)* - The green-colored regions highlight weak, non-covalent interactions, such as van der Waals forces (London dispersion and dipole-dipole interactions). These interactions, characterized by sign(λ_2)ρ values close to zero, are predominantly observed between the carbon-hydrogen (C–H) bonds of Captagon's phenyl rings and the graphene surface, as well as between heteroatoms in Captagon and the underlying graphene sheet. Despite their relatively weak nature, these interactions contribute significantly to the overall adsorption of Captagon onto graphene, stabilizing the π–π stacking arrangement.

3.4. *Calculations via the general utility lattice program (GULP)*

The general utility lattice program (GULP) software is highly efficient for studying large atomic systems, where DFT becomes impractical due to its

high computational cost. In this study, we employed this approach to evaluate how Captagon interacts when adsorbed (sandwiched) between two graphene layers in a large system ($C_{158}H_{22}N_5O_2$).

As shown in Figure 7, the Captagon molecule interacts efficiently within the layers. The interlayer distance of graphene, when Captagon is inserted, is 7.136 Å. Additionally, the atomic distances within Captagon indicate strong interactions with both graphene layers, comparable to those observed in DFT calculations.

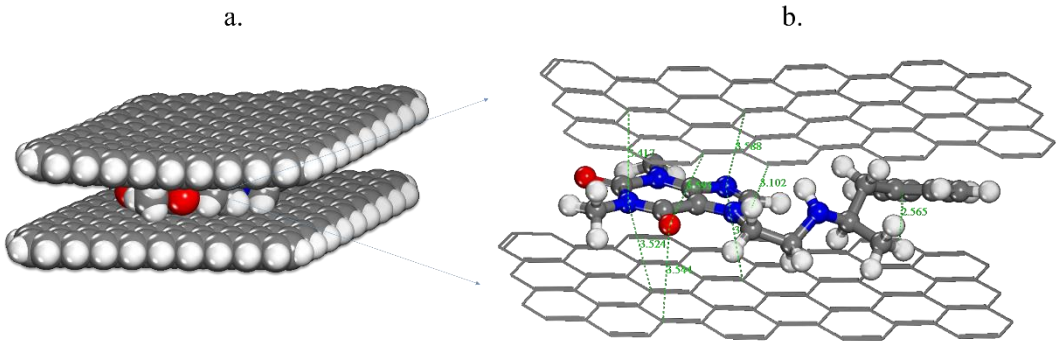

Fig. 7. Optimized geometry (and some corresponding adsorption distances) for the 'sandwich' interaction of Captagon between two layers of graphene.

4. CONCLUSION

This study explored the adsorption potential of graphene for removing Captagon (fenethylline) from contaminated environments using computational chemistry techniques, including density functional theory (DFT), Monte Carlo (MC), and molecular dynamics (MD) simulations. The results indicate that graphene exhibits strong adsorption potential for Captagon, particularly in a parallel configuration, where π–π stacking interactions significantly enhance adsorption stability.

Monte Carlo simulations demonstrated that Captagon adsorption onto graphene is more favorable in aqueous environments than in a vacuum, with interaction energies suggesting thermodynamically stable binding. The presence of water molecules further stabilized the adsorption process. Molecular dynamics simulations confirmed the persistent interaction between Captagon and graphene over time, reinforcing graphene's suitability as an adsorbent for drug removal applications.

DFT calculations revealed significant changes in the electronic properties of graphene upon Captagon adsorption, including shifts in E_{HOMO}, E_{LUMO}, and bandgap (E_{gap}), further highlighting the strong electronic interaction between the two systems. Analysis of atomic charge distributions confirmed that electronegative atoms, particularly oxygen and nitrogen, serve as primary adsorption sites, strengthening graphene's adsorption capabilities.

Moreover, general utility lattice program (GULP) simulations demonstrated the feasibility of Captagon entrapment between graphene layers, further expanding graphene's potential as a material for adsorption-based filtration technologies. These findings underscore graphene's promise as an effective adsorbent for Captagon removal, with broader implications for environmental remediation.

Conflict of interest. The authors declare that they have no known financial or personal relationships that could have appeared to influence the work reported in this paper. No competing interests exist regarding the publication of this study.

Acknowledgements. The authors gratefully acknowledge the Ministry of Education, Science, Technology, and Innovation (MESTI) of Kosovo for providing the computing resources necessary for this study. Their support has been instrumental in facilitating the simulations and analyses presented in this work.

REFERENCES

[1] Al Omari, O; Wynaden, D; Alkhawaldeh, A.; Alhalaiqa, F.; Al Dameery, K.; Roach, E. J.; Sunderraj, S. J.; Khalaf, A., Jordanian University students' lived experience of misusing amphetamine (Captagon): A qualitative study, *J. Addict. Nurs.* **2022**, *33*, 20–26. https://doi.org/10.1097/JAN.0000000000000446

[2] Elasfar, A. A.; Ahmad, K. E.; Al Shaghaa, W., Clinical characteristics and outcome of heart failure and captagon amphetamine use: An observational prospective study, *Egypt. Hear. J.* **2014**, *66*, 5. https://doi.org/10.1016/j.ehj.2013.12.015

[3] Abazid, H., Drug abuse in the Middle East: A focus on Syria, *Handb. Subst. Misuse Addict. from Biol. to Public Heal*. **2022**, 2629–2648. https://doi.org/10.1007/978-3-030-92392-1_140

[4] Fong, S.; Carollo, A.; Rossato, A.; Prevete, E.; Esposito, G.; Corazza, O., Captagon: A comprehensive bibliometric analysis (1962–2024) of its global impact, health and mortality risks, *Saudi Pharm. J.* **2024**, *32*, 102188. https://doi.org/10.1016/J.JSPS.2024.102188

[5] Al-Imam, A.; Santacroce, R.; Roman-Urrestarazu, A.; Chilcott, R.; Bersani, G.; Martinotti, G.; Corazza, O., Captagon: use and trade in the Middle East, *Hum. Psychopharmacol. Clin. Exp*. **2017** *32*, e2548. https://doi.org/10.1002/HUP.2548

[6] Ogwu, M.C.; Malík, M.; Tlustoš, P.; Patočka, J. The Psychostimulant Drug, Fenethylline (Captagon):Health Risks, Addiction and the Global Impact of Illicit Trade. Drug Alcohol Depend. Reports **2025**, *15*, 100323, DOI:10.1016/J.DADR.2025.100323.

[7] Katselou, M.; Papoutsis, I.; Nikolaou, P.; Qammaz, S.; Spiliopoulou, C.; Athanaselis, S., Fenethylline (Captagon) Abuse – Local Problems from an Old Drug Become Universal, *Basic Clin. Pharmacol. Toxicol*. **2016**, *119*, 133–140. https://doi.org/10.1111/BCPT.12584

[8] Jr, J.P.; LeQuang, J.A.K.; Vortsman, E.; Magnusson, P.; EL-Tallawy, S. N.; Wagner, M.; Salah, R.; Varrassi, G., The emergence of the old drug captagon as a new ıllicit drug: A narrative review, *Cureus.* **2024**, *16*. https://doi.org/10.7759/CUREUS.55053

[9] Geim, A. K.; Novoselov, K. S.; The rise of graphene, *Nat. Mater*. **2007**, *63*, (6), 183–191. https://doi.org/10.1038/nmat1849

[10] Urade, A. R.; Lahiri, I.; Suresh, K. S.; Graphene properties, synthesis and applications: A review, *JOM* **2023**, *75*, 614–630. https://doi.org/10.1007/S11837-022-05505-8

[11] Allen, M. J.; Tung, V. C.; Kaner, R. B., Honeycomb carbon: A review of graphene, *Chem. Rev*., **2010**, *110*, 132–145. https://doi.org/10.1021/CR900070D/ASSET/CR900070D.FP.PNG_V03

[12] Li, Y.; Nie, Y.; Zhou, J., The development of graphene and ıts use in flexible electronics, *Highlights Sci. Eng. Technol.* **2022**, *27*, 798–805. https://doi.org/10.54097/hset.v27i.3848

[13] Pumera, M., Graphene-based nanomaterials and their electrochemistry, *Chem. Soc. Rev*. **2010**, *39*, 4146. https://doi.org/10.1039/c002690p

[14] Berisha, A., Density functional theory and quantum mechanics studies of 2D carbon nanostructures (graphene and graphene oxide) for Lenalidomide anticancer drug delivery, *Comput. Theor. Chem*. 1230 **2023**. https://doi.org/10.1016/j.comptc.2023.114371

[15] Mehmeti, V.; Halili, J.; Berisha, A., Which is better for Lindane pesticide adsorption, graphene or graphene oxide? An experimental and DFT study, *J. Mol. Liq*. **2022**, *347*. https://doi.org/10.1016/j.molliq.2021.118345

[16] Yang, K.; Feng, L.; Shi, X.; Liu, Z., Nano-graphene in biomedicine: theranostic applications, *Chem. Soc. Rev*. **2012**, *42*, 530–547. https://doi.org/10.1039/C2CS35342C

[17] Belletto, D.; Vigna, V.; Barretta, P.; Ponte, F.; Mazzone, G.; Scoditti, S.; Sicilia, E., Computational assessment of the use of graphene-based nanosheets as PtII chemo-therapeutics delivery systems, *J. Comput. Chem*. **2024**, *45*, 2059–2070. https://doi.org/10.1002/JCC.27394

[18] Zhou, Y.; Li, H.; Zhang, J.; Wu, Y.; Zheng, P.; Jiang, Y.; Stylianakis, M.; Skouras, A.; Gong, P.; Zhou, Y.; Li H.; Zhang, J.; Wu, Y.; Zheng, P.; Jiang, Y., Theoretical study on the aggregation and adsorption behaviors of anticancer drug molecules on graphene/graphene oxide surface, *Mol*. **2022**, Vol. *27*, Page 6742. https://doi.org/10.3390/MOLECULES27196742

[19] Peng, B.; Chen, L.; Que, C.; Yang, K.; Deng, F.; Deng, X.; Shi, G.; Xu, G.; Wu M., Adsorption of antibiotics on graphene and biochar in aqueous solutions ınduced by π-π interactions, *Sci. Reports* **2016**, *61*, 6 (2016) 1–10. https://doi.org/10.1038/srep31920

[20] Mehmeti, V.; Sadiku, M., A comprehensive DFT investigation of the adsorption of polycyclic aromatic hydrocarbons onto graphene, *Computation*. **2022**, *10*, 68. https://doi.org/10.3390/computation10050068

[21] Kim, S.; Chen, J.; Cheng, T.; Gindulyte, A.; He, J.; He, S.; Li, Q.; Shoemaker, B. A.; Thiessen, P. A.; Yu, B.; Zaslavsky, L.; Zhang, J.; Bolton, E. E.; *PubChem update*, *Nucleic Acids Res*. **2025**, *53*, D1516–D1525. https://doi.org/10.1093/nar/gkae1059

[22] Neese, F.; Wennmohs, F.; Becker, U.; Riplinger, C., The ORCA quantum chemistry program package, *J. Chem. Phys.* **2020**, *152*, 224108. https://doi.org/10.1063/5.0004608/1061982

[23] Neese F., Software update: The ORCA program system — Version 5.0, *Wiley Interdiscip. Rev. Comput. Mol. Sci*. **2022**, *12*, e1606. https://doi.org/10.1002/WCMS.1606

[24] Neese, F., Software update: the ORCA program system, version 4.0, *WIREs Comput. Mol. Sci.* **2018**, *8*, e1327. https://doi.org/10.1002/wcms.1327

[25] Grimme, S.; Bannwarth, C.; Shushkov, P., A robust and accurate tight-binding quantum chemical method for structures, vibrational frequencies, and noncovalent ınteractions of large molecular systems parametrized for all spd-block elements (Z = 1–86), *J. Chem. Theory Comput*. **2017**, *13*, 1989–2009. https://doi.org/10.1021/ACS.JCTC.7B00118/ASSET/IMAGES/LARGE/CT-2017-001185_0011.JPEG

[26] Mayo, S. L.; Olafson, B. D.; Goddard, W. A., DREIDING: a generic force field for molecular simulations, *J. Phys. Chem*. **1990**, *94*, 8897–8909. https://doi.org/10.1021/j100389a010

[27] Evans, D. J.; Holian, B. L., The Nose-Hoover thermostat, *J. Chem. Phys*. **985**, *83* (1), 4069–4074. https://doi.org/10.1063/1.449071

[28] Delley, B., An all-electron numerical method for solving the local density functional for polyatomic molecules, *J. Chem. Phys.* **1990**, *92*, 508–517. https://doi.org/10.1063/1.458452

[29] Delley, B., From molecules to solids with the DMol3 approach, *J. Chem. Phys.* **2000**, *113*, 7756–7764. https://doi.org/10.1063/1.1316015

[30] Peverati, R.; Truhlar, D. G., M11-L: A local density functional that provides improved accuracy for electronic structure calculations in chemistry and physics, *J. Phys. Chem. Lett*. **2012**, *3*, 117–124. https://doi.org/10.1021/JZ201525M/SUPPL_FILE/JZ201525M_SI_001.PDF

[31] Pulay, P., Convergence acceleration of iterative sequences. the case of scf iteration, *Chem. Phys. Lett*. 73 (1980) 393–398. https://doi.org/10.1016/0009-2614(80)80396-4

[32] Gale, J. D.; Rohl, A. L., The General Utility Lattice Program (GULP), *Mol. Simul*. **2003**, *29*, 291–341. https://doi.org/10.1080/0892702031000104887

[33] Gale, J. D., GULP: A computer program for the symmetry-adapted simulation of solids, *J. Chem. Soc. Faraday Trans.* **1997**, *93*, 629–637. https://doi.org/10.1039/A606455H

[34] Senftle, T. P.; Hong, S.; Islam, M. M.; Kylasa, S. B.; Zheng, Y.; Shin, Y. K.; Junkermeier, C.; Engel-Herbert, R.; Janik, M. J.; Aktulga, H. M.; Verstraelen, T.; Grama, A.; Van Duin, A. C. T., The ReaxFF reactive force-field: Development, applications and future directions, *Npj Comput. Mater*. **2016**, *21*, 2, 1–14. https://doi.org/10.1038/npjcompumats.2015.11

[35] Thoume, A.; Benmessaoud Left, D.; Elmakssoudi, A.; Safi, Z. S.; Benzbiria, N.; Berisha, A.; Kellal, R.; Zertoubi, M. An In-Depth on the High Corrosion Resistance of Carbon Steel in an Acidic Solution by a Novel Functionalized Graphene Oxide with Oxime Derivative via Cutting-Edge Experimental Characterization and Computational Modeling. *Mater. Chem.* Phys. **2023**, *310*. DOI:10.1016/j.matchemphys.2023.128487

[36] Khalaf, B.; Hamed, O.; Jodeh, S.; Bol, R.; Hanbali, G.; Safi, Z.; Dagdag, O.; Berisha, A.; Samhan, S., Cellulose-based hectocycle nanopolymers: synthesis, molecular docking and adsorption of difenoconazole from aqueous medium, *Int. J. Mol. Sci*. **2021**, *22*. https://doi.org/10.3390/ijms22116090

[37] Ajebli, S.; Kaichouh, G.; Khachani, M.; Babas, H.; El Karbane, M.; Warad, I.; Safi, Z. S.; Berisha, A.; Mehmeti, V.; Guenbour, A.; Bellaouchou, A.; Zarrouk, A., The adsorption of Tenofovir in aqueous solution on activated carbon produced from maize cobs: Insights from experimental, molecular dynamics simulation, and DFT calculations, *Chem. Phys. Lett*. **2022**, *801*, 139676. https://doi.org/10.1016/j.cplett.2022.139676

[38] Haziri, V.; Berisha, A.; Haliti, M.; Kaya, S.; Thaçi, V.; Seydou, M., Exploring the mechanism of nerve agent (Tabun and Sarin) adsorption on carbon nanocones: Computational insights, *J. Mol. Liq.* **2024**, *407*, 125176. https://doi.org/10.1016/J.MOLLIQ.2024.125176

[39] Azzaoui, K.; Aaddouz M., Akartasse, N.; Mejdoubi, E.; Jodeh, S.; Hammouti, B.; Taleb, M., ES-Sehli, S.; Berisha, A.; Rhazi, L.; Lamhamdi, A.; Algarra, M., Synthesis of β-tricalcium phosphate/PEG 6000 composite by novel dissolution/precipitation method: Optimization of the adsorption process using a factorial design — DFT and molecular dynamic, Arab. *J. Sci. Eng*. **2024**, *49*, 711–732. https://doi.org/10.1007/S13369-023-08390-8/METRICS

[40] El Gaayda, J.; Ezzahra Titchou, F.; Oukhrib, R.; Karmal, I.; Abou Oualid, H.; Berisha, A.; Zazou, H.; Swanson, C.; Hamdani, M.; Ait Akbour, R.; Removal of cationic dye from coloured water by adsorption onto hematite-humic acid composite: Experimental and theoretical studies, *Sep. Purif. Technol*. **2022**, *288*, 120607. https://doi.org/10.1016/j.seppur.2022.120607

[41] Ulusoy, S.; Akalin, R. B.; Çevikbaş, H.; Berisha, A.; Oral, A.; Boşgelmez-Tinaz, G., Zeolite 4A as a jammer of bacterial communication in *Chromobacterium violaceum* and *Pseudomonas aeruginosa*, *Future Microbiol.* **2022**, *17*. https://doi.org/10.2217/FMB-2021-0174

[42] Rub, H. A.; Deghles, A.; Hamed, O.; Azzaoui, K.; Hammouti, B.; Taleb, M.; Berisha, A.; Dagdag, O.; Mansour, W.; Hacıosmanoğlu, G. G.; Can, Z. S.; Rhazi, L., Cellulose based polyurethane with amino acid functionality: Design, synthesis, computational study and application in wastewater purification, *Int. J. Biol. Macromol***. 2023**, *239*. https://doi.org/10.1016/j.ijbiomac.2023.124328

[43] Sadiku, M.; Selimi, T.; Berisha, A.; Maloku, A.; Mehmeti, V.; Thaçi, V.; Hasani, N., Removal of methyl violet from aqueous solution by adsorption onto halloysite nanoclay: experiment and theory, *Toxics* **2022**, *10*, 445. https://doi.org/10.3390/TOXICS10080445

[44] El Mouden, A.; El Messaoudi, N.; El Guerraf, A.; Bouich, A.; Mehmeti, V.; Lacherai, A.; Jada, A.; Pinê Américo-Pinheiro, J. H., Removal of cadmium and lead ions from aqueous solutions by novel dolomite-quartz@Fe_3O_4 nanocomposite fabricated as nano-adsorbent, *Environ. Res*. **2023**, *225*. https://doi.org/10.1016/j.envres.2023.115606

[45] Jodeh, S.; Jaber, A.; Hanbali, G.; Massad, Y.; Safi, Z. S.; Radi, S.; Mehmeti, V.; Berisha, A.; Tighadouini, S.; Dagdag, O., Experimental and theoretical study for removal of trimethoprim from wastewater using organically modified silica with pyrazole-3-carbaldehyde bridged to copper ions, *BMC Chem*. **2022**, *16*. https://doi.org/10.1186/s13065-022-00814-0

[46] Mehmeti, V.; Sadiku, M., A Comprehensive DFT ınvestigation of the adsorption of polycyclic aromatic hydrocarbons onto graphene, *Computation*. **2022**, *10*. https://doi.org/10.3390/computation10050068

[47] Javaid, S.; Lee, G., The impact of molecular orientation on carrier transfer characteristics at a phthalocyanine and halide perovskite interface, *RSC Adv*. **2021**, *11*, 31776. https://doi.org/10.1039/D1RA05909B

[48] Lazar, P.; Karlický, F.; Jurecka, P.; Kocman, M.; Otyepková, E.; Šafářová, K.; Otyepka, M., Adsorption of small organic molecules on graphene, *J. Am. Chem. Soc*. **2013**, *135* 6372–6377. https://doi.org/10.1021/JA403162R

[49] Hellal, A.; Abdelsalam, H.; Tawfik, W.;. Ibrahim, M. A, Assessment of doped graphene in the removal of atrazine from water, *Sci. Reports* **2024**, 141, 14, 1–17. https://doi.org/10.1038/s41598-024-71886-2

[50] Zhan, J.; Lei, Z.; Zhang, Y. Non-Covalent Interactions of Graphene Surface: Mechanisms and Applications. *Chem* **2022**, *8*, 947–979. DOI:10.1016/J.CHEMPR.2021.12.015

[51] Pérez, E. M.; Martín, N., π–π interactions in carbon nanostructures, *Chem. Soc. Rev*. **2015**, 44, 6425–6433. https://doi.org/10.1039/C5CS00578G

[52] Johnson, E. R.; Keinan, S.; Mori-Sánchez, P.; Contreras-García, J.; Cohen, A. J.; Yang, W., Revealing noncovalent interactions, *J. Am. Chem. Soc*. **2010**, *132*, 6498–6506. https://doi.org/10.1021/JA100936W/SUPPL_FILE/JA100936W_SI_002.PDF

[53] Lu, T.; Chen, F., Multiwfn: A multifunctional wavefunction analyzer, *J. Comput. Chem*. **2012**, *33*, 580–592. https://doi.org/10.1002/jcc.22885

[54] Humphrey, W.; Dalke, A.; Schulten, K., VMD: visual molecular dynamics, *J. Mol. Graph*. **1996**, *14*, 33–38. https://doi.org/10.1016/0263-7855(96)00018-5

[55] Berisha, A., The influence of the grafted aryl groups on the solvation properties of the graphyne and graphdiyne-A MD study, *Open Chem*. **2019**, *17*, 703–710. https://doi.org/10.1515/chem-2019-0083

[56] Berisha, A., Interactions between the aryldiazonium cations and graphene oxide: A DFT study, *J. Chem*. **2019**. https://doi.org/10.1155/2019/5126071

[57] Halili, J.; Berisha, A.; Halili, J.; Berisha, A., An experimental and theoretical analysis of supercritical carbon dioxide extraction of Cu(II) and Pb(II) ions in the form of dithizone bidentate complexes, *Turkish J. Chem*. **2022**, *46*, 721–729. https://doi.org/10.55730/1300-0527.3362

[58] Berisha, A. Unraveling the Electronic Influence and Nature of Covalent Bonding of Aryl and Alkyl Radicals on the B12N12 *Nanocage Cluster*. *Sci. Rep*. **2023**, *13*. DOI:10.1038/s41598-023-28055-8